Molecular Crystals and Liquid Crystals
Publication details, including instructions for authors and subscription information:
http://www.tandfonline.com/loi/gmcl20

# Transparent Thin Films of Anatase Titania Nanoparticles with High Refractive Indices Prepared by Wet Coating Process

Young Gon Seo [a], Hyunjung Lee [b], Kyungkon Kim [b] & Wonmok Lee [a]
[a] Department of Chemistry, Sejong University, Gwangjin-gu, Seoul, Korea
[b] Materials Science and Technology Research Division, Korea Institute of Science and Technology, Seongbuk-gu, Seoul, Korea

Version of record first published: 19 Apr 2010

To cite this article: Young Gon Seo, Hyunjung Lee, Kyungkon Kim & Wonmok Lee (2010): Transparent Thin Films of Anatase Titania Nanoparticles with High Refractive Indices Prepared by Wet Coating Process, Molecular Crystals and Liquid Crystals, 520:1, 201/[477]-208/[484]

To link to this article: http://dx.doi.org/10.1080/15421400903584424

*Mol. Cryst. Liq. Cryst.*, Vol. 520: pp. 201/[477]–208/[484], 2010

ISSN: 1542-1406 print/1563-5287 online
DOI: 10.1080/15421400903584424

Taylor & Francis
Taylor & Francis Group

# Transparent Thin Films of Anatase Titania Nanoparticles with High Refractive Indices Prepared by Wet Coating Process

YOUNG GON SEO,[1] HYUNJUNG LEE,[2]
KYUNGKON KIM,[2] AND WONMOK LEE[1]

[1]Department of Chemistry, Sejong University, Gwangjin-gu, Seoul, Korea
[2]Materials Science and Technology Research Division, Korea Institute of Science and Technology, Seongbuk-gu, Seoul, Korea



*We present a sol-gel derived anatase titania nanoparticle system which can be spin-coated to form thin films having high refractive index and excellent optical clarity. Stable titania suspensions were obtained through peptization of crude product in the presence of tetramethylammonium hydroxide. The particle sizes and morphologies were finely controlled by mild hydrothermal treatment at 200°C. Three titania suspensions obtained by different hydrothermal reaction time showed stable suspensions without significant flocculation, and subsequently spin coated on the glass substrates. Without calcinations step, the resulting films exhibited fairly good optical clearance and refractive indices as high as 2.05. Narrow dispersity of the particle size and the stability of titania suspension also enabled the fabrication of inverse opal structure by templating method which could be further utilized as various applications such as photonic bandgap materials and photoelectrode for solar cells.*

**Keywords** Anatase; hydrothermal reaction; inverse opal; solution process; thin film; titania nanoparticle; transparent

## Introduction

Sol-gel syntheses are well known routes for the preparation of metal oxide nanoparticles which provide low polydispersity and high crystallinity. An important advantage of sol-gel synthesis is that the particle size and the morphology can be controlled by experimental conditions [1,2]. In particular, sol-gel processed titania ($TiO_2$) has attracted a lot of attention due to its potential for various applications such as solar cell [3,4], photocatalysis [5,6], antibacterial coating [7], and photonic crystal [5]. Depending on synthetic routes and post-thermal treatment conditions, three different crystalline phases of $TiO_2$ are found: brookite, anatase, and rutile. Although rutile is denser and has greater refractive index, anatase phase shows the most efficient electron mobility and thus is most preferred for solar cell applications [4]. Thin films of nanocrystalline $TiO_2$ can be obtained either by dry-process or

Address correspondence to Wonmok Lee, Department of Chemistry, Sejong University, 98 Gunja-Dong, Gwangjin-gu, Seoul 143-747, Korea. Tel.: +82-2-3408-3212; Fax: +82-2-462-9954; E-mail: wonmoklee@sejong.ac.kr

wet-process. Compared to the dry-process such as a vacuum sputtering which requires a bulky apparatus with high vacuum and high purity target [8], wet-coating process of sol-gel derived $TiO_2$ nanoparticles dispersed in liquid matrix provides an excellent flexibility from the process point of view [9]. In order to improve crystallinity of wet-coated $TiO_2$ thin film, the post thermal treatments on the films are often followed [4]. However, the post thermal process can be avoided if the synthesized $TiO_2$ nanoparticles are highly crystalline. The quality of the coated film strongly depends on the stability of the suspension. Peptization process is a good way to yield a highly stable $TiO_2$ suspension in water. In peptization, adsorption of salt ions such as tetramethylammonium hydroxide occurs on the surface of $TiO_2$ nanoparticles which exert electrostatic repulsion between the particles to prevent flocculation. By introducing various peptizing agent, aggregation of $TiO_2$ nanoparticles can be minimized and the crystallinity can be increased [10]. Highly crystalline $TiO_2$ nanoparticles can be prepared by hydrothermal reaction of $TiO_2$ sol. In hydrothermal process, reaction condition is controlled by temperature-driven autonomic pressure from the solvent in a sealed reactor which converts $TiO_2$ sol to highly crystalline suspension [11]. Although rutile phase is thermodynamically more stable, anatase is more often found in sol-gel syntheses of $TiO_2$ due to kinetic reasons [12]. Yang *et al.* reported that the peptization at a low pH promotes the formation of rutile phase, while basic peptizing agent such as tetraalkylammonium hydroxide generally results in anatase phase [13]. Jeon *et al.* prepared a rare-earth doped $TiO_2$ nanoparticles for photonic application by peptization with tetraalkylammonium hydroxide followed by hydrothermal synthesis [11]. They observed pure anatase $TiO_2$ nanoparticles, and the suspensions were wet-coated, and thermally treated to further improve refractive index. For photonic application, high refractive index is an important physical property. However, it would be advantageous if thermal treatment step is removed from the process point of view. In this study, we investigated mild hydrothermal reaction conditions in order to control the particle size and the crystallinity of the peptized $TiO_2$ nanoparticle system while maintaining transparency of the coated films. Colloidal suspension of pure $TiO_2$ nanoparticle without organic additives was confirmed to have multiple advantages toward thin film processes. Rigorous characterizations on the nanoparticles and the final films were carried out.

## Experimental

The $TiO_2$ nanoparticle sol was synthesized by following procedure. 3 ml of Titanium isopropoxide ($Ti(i\text{-}PrO)_4$, TCI) was added dropwise in 54 mL of DI water. After the mixture was stirred for 1 hours, crude product was purified with DI water three times, and the sediment was mixed with 15 mL DI water and 1 mL tetramethylammonium hydroxide (TMNOH, 25% in water, TCI). The turbid dispersion was peptized for 24 hours at 85°C. At the end of peptization, $TiO_2$ sol became transluscent.

As-synthesized $TiO_2$ nanoparticle sol was directly subjected to mild hydrothermal reaction as following. 20 mL of $TiO_2$ dispersion in water was added in 40 mL Teflon liner, which was tightly sealed in a stainless steel bomb reactor (4744, Parr instrument). In a temperature stabilized oven, mild hydrothermal reaction was carried out at 200°C, for different period of time. Upon completion of the hydrothermal treatment, the respective dispersion was centrifuged at 10000 rpm. The supernatant was decanted and the transluscent sediments were redispersed in DI water.

The washing process for $TiO_2$ nanoparticle was repeated several times until fishy odor disappears.

The $TiO_2$ thin films were obtained by spin coating the dispersions on the flat substrate. The microscope slide glass and the silicon substrate were cleaned by freshly prepared piranha solution (3/1 volume mixture of $H_2SO_4/H_2O_2$), and rinsed with DI water several times. The $TiO_2$ dispersions were spin coated on the cleaned substrate at 2000 rpm. After spin coating, the films were dried in convection oven at 70°C. The thicknesses and the refractive indices of the $TiO_2$ thin films were characterized by ellipsometry (SE MF-1000, Nano-view) and the film morphologies were analyzed by scanning electron microscopy (SEM, Hitachi S-4700) without calcinations.

The crystal structure of dried $TiO_2$ powder was characterized by X-ray diffractometer (XRD, Rigaku D/Max-2500) operating with Cu-K$\alpha$ radiation. The full width at half maximum (FWHM) of the characteristic peaks in each X-ray diffractogram were measured and the average particle sizes were calculated by applying Scherrer equation.

For the fabrication of $TiO_2$ inverse opal structure, the colloidal crystal template was prepared by using narrowly dispersed poly(methylmethacrylate) (PMMA) microspheres with 240 nm particle size. The PMMA microsphere was synthesized by typical emulsion polymerization as reported elsewhere [14]. The aqueous PMMA dispersion was drop-cast on a glass substrate, and slowly dried in a closed petri dish. Resulting opal structure of PMMA showed a shiny iridescence upon reflection of light. Onto the dried PMMA opal, an as synthesized $TiO_2$ suspension was added dropwise, and dried in air for 24 hours. The infiltrated opal was calcined in a furnace at 450°C for 2 hours to generate $TiO_2$ inverse opal, which was characterized by SEM.

## Results and Discussion

In this study, the pristine $TiO_2$ nanoparticle was obtained by simple hydrolysis of $Ti(i\text{-}PrO)_4$ in water. The crude product was white $TiO_2$ cake which was directly subject to peptization process. Once peptized in the presence of TMNOH, white $TiO_2$ suspension turned clear as shown in Figure 1(a), which implies $TiO_2$ nanoparticles

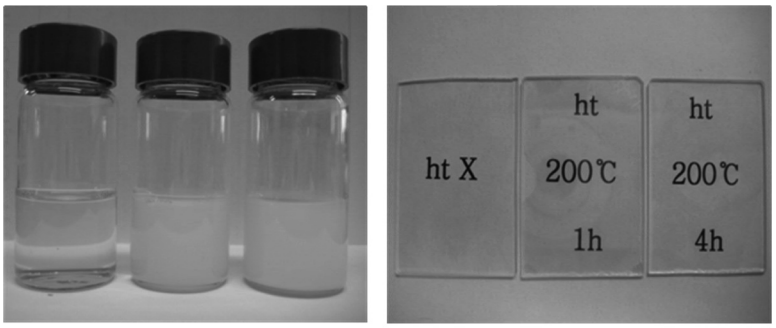


(a) (b)

**Figure 1.** (a) Non-aggregated titania nanoparticles suspensions in water; from left, as-peptized $TiO_2$, after hydrothermal reaction for 1 hour, and 4 hours. Each suspension contained 6.4, 6.3, 4.1wt % of $TiO_2$ nanoparticles respectively. (b) Thin films of $TiO_2$ by spin coating of three suspensions at 2000 rpm.

are well dispersed without flocculation. Such a stable suspension was further treated by hydrothermal reaction at a fixed reaction temperature of 200°C. Then, we varied the hydrothermal reaction time to obtain the nanoparticles with an increased particle size and a crystallinity as well without deteriorating transparency of the coated film. It was confirmed that the hydrothermal reaction less than 5 hours results in translucent suspensions which can consequently form the transparent thin films upon spin coating. Longer reaction time caused turbid suspension which resulted in an opaque film. In order to avoid an opaque film, we prepared three $TiO_2$ suspensions by hydrothermal reaction for 0 hour (no hydrothermal reaction), 1 hour and 4 hours. The hydrothermally treated suspensions were somewhat turbid as shown in Figure 1(a). However, all three suspensions resulted in optically clear films upon spin coating on the glass substrate as shown in Figure 1(b). The opaqueness in suspension is partly attributed to be the high refractive index of the nanoparticles which strongly scattered visible light.

Figure 2 shows the SEM images of the top surfaces of the films shown in Figure 1(b). All the films showed even surfaces without crack, and individual nanoparticles could be distinguished due to their finite particle sizes. Compared to Figure 2(a) where relatively small nanoparticles are shown, Figures 2(b) and (c) show the gradual increases in $TiO_2$ particle sizes by longer hydrothermal reaction time. It is well known that the hydrothermal reaction increases crystallinity and particle size at the same time [11]. Overall particle shapes were elliptical, though some particles were appeared to be irregularly shaped. Nevertheless, the size distributions for all three cases were quite narrow which are responsible for optical clarity and transparency of the films.

For the characterization of crystal morphologies of $TiO_2$ nanoparticles, the dried powders were analyzed by XRD. Figure 3 shows the diffractograms of $TiO_2$ nanoparticles exhibiting characteristic peaks from anatase crystal. As shown in the figure, broad diffraction peaks become narrower, and thus the overlapped peaks become separated as hydrothermal reaction time increased. Closer look at the diffractogram of the as-synthesized $TiO_2$ shows weak diffraction peak from brookite as indicated by arrow in the Figure. However, such a trace amount of brookite phase disappeared once the hydrothermal treatment was carried out. It is clearly shown that the $TiO_2$ nanoparticles after 4 hours of hydrothermal reaction at 200°C exhibited no trace of brookite peak. Therefore, it was confirmed that the hydrothermal condition in this study was appropriate for the preparation of anatase $TiO_2$.

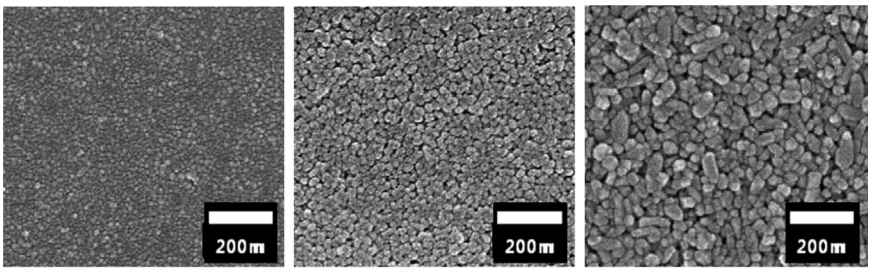


**Figure 2.** SEM images of the $TiO_2$ films prepared at the different hydrothermal reaction time. (a) 0 hour, (b) 1 hour, and (c) 4 hours.

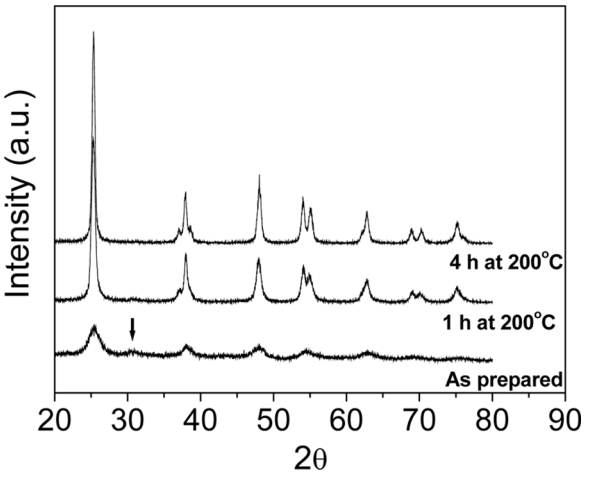


**Figure 3.** Powder X-ray diffractograms of $TiO_2$ samples obtained at different hydrothermal reaction time. The arrow indicates a trace of brookite crystal before hydrothermal treatment.

By measuring full width half maximum (FWHM) of the peaks from (101), (004), (200), (204), and (215) anatase plane, average particle size ($d_{ave}$) of each $TiO_2$ nanoparticle was calculated based on Scherrer formula, and the calculated sizes are summarized in Table 1. The calculated $d_{ave}$ clearly showed the increasing tendency of the particle size from 9 nm to 30 nm by increased hydrothermal reaction time. It is noteworthy that the particle size increased 160% by short hydrothermal treatment. It was found in this study that a longer hydrothermal reaction time did not cause substantial increase in the particle size as shown in the Table 1, but the particle size distribution became broader which is undesirable for the purpose of this study. Although not shown, we also carried out hydrothermal reaction for 10 h on the same $TiO_2$ suspension, which resulted in a particle size increased only upto 33 nm. However, the thin film from the 10 h-treated suspension was too opaque due to an existence of large $TiO_2$ particles and their agglomerates.

In order to characterize the film thicknesses and refractive indices of the $TiO_2$ films, each dispersion shown in Figure 1(a) was spin-coated on the Si wafer which had been pre-cleaned by piranha treatment. All the coated $TiO_2$ films were optically clean without dewetting or any visible aggregates, exhibiting shiny metallic color depending on the thickness. Thin film samples on Si wafer were subjected to an ellipsometry with a fixed angle (69°) for measuring refractive indices and film thicknesses. In this study, we aimed to obtain optically clear, solution-processible $TiO_2$ nanoparticle system having increased refractive index without calcinations at high

**Table 1.** Physical properties of $TiO_2$ nanoparticles and thin films

| Hydrothermal time | 0 h | 1 h | 4 h |
|---|---|---|---|
| Average size (nm) | 9 | 24 | 30 |
| Refractive index (@ 500 nm) | 1.77 | 2.02 | 2.05 |
| Film thickness (nm) | 116 | 93 | 66 |

temperature. Thus, thin film samples were analyzed right after drying at 70°C making fabrication process simple. Figure 4 shows the changes in refractive index of the film as the hydrothermal reaction time is increased. $TiO_2$ by 10 hours of hydrothermal reaction is not shown since the film was not adequate for ellipsometry analysis due to opaqueness. However, 4 hours hydrothermal reaction did not cause opaqueness to the coated film. Although the refractive index of the as-peptized $TiO_2$ is only 1.77, hydrothermal reaction caused the increase in the refractive index as high as 2.05. It is noteworthy that the refractive index of $TiO_2$ film exceeded 2.0 without calcination. Consequently, it was confirmed that the optimized synthesis $TiO_2$ nanoparticles resulted in a stable aqueous suspension, which provided a transparent films with high refractive index by spin coating without thermal treatment at high temperature.

Excellent solution processibility of our $TiO_2$ nanoparticle system allows another exciting application. There have been reports on the inverse opal $TiO_2$ which is a promising photonic bandgap material. Inverse opal is formed by infiltration of a secondary material in opal template, which is often called colloidal crystal, followed by removal of the template structure. Since air voids are inverted by those processes, the resulting structure is called inverse opal. In general, the inverse opal $TiO_2$ films are prepared by infiltration of $TiO_2$ sol followed by calcination, which usually involves serious cracks by volume shrinkage from the elimination of water by condensation reaction of precursors. On the other hand, our system does not suffer from a serious shrinkage problem since we use an already-formed $TiO_2$ nanoparticle which barely contains unreacted precursor, and thus the crack is minimized in the final inverse opal structure. Figure 5 demonstrates a typical SEM image of the fractured sample of $TiO_2$ inverse opal structure. An enlarged view in Figure 5(b) shows the holes in the inverse opal cavities, which are the contact points (necking) between PMMA microspheres before calcinations. Ordered mesoporous structures of $TiO_2$ such as inverse opal can promise various photonic bandgap applications due to high refractive index [15]. Furthermore, anatase $TiO_2$ inverse opal structure can be utilized as an efficient photoelectrode for dye sensitized solar cell [4]. Taking such advantages

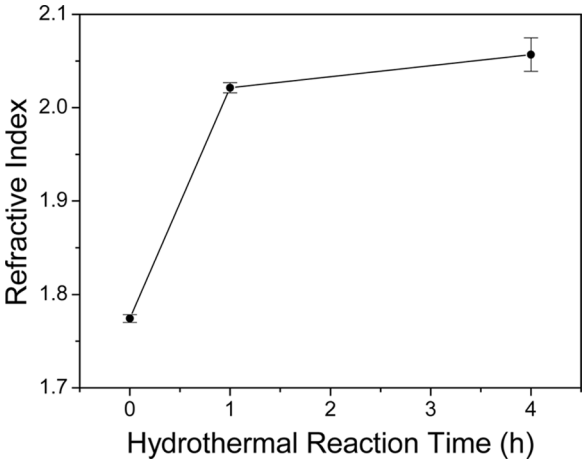


**Figure 4.** Refractive indices of $TiO_2$ thin films spin-coated on Si wafer by different reaction time, and the measurement was carried out using ellipsometry.

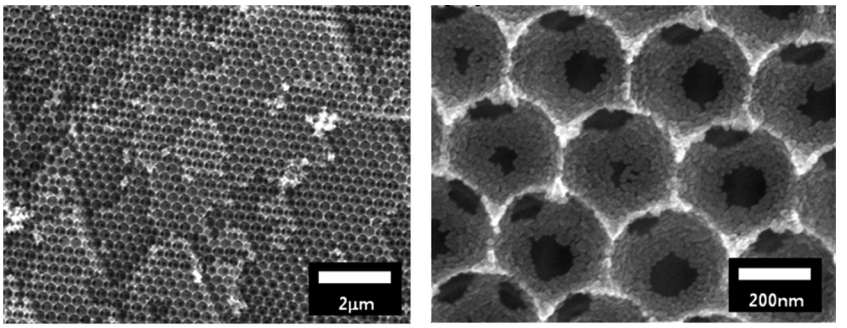


(a) (b)

**Figure 5.** SEM images showing inverse opal photonic crystal structure of $TiO_2$ nanoparticles infiltrated within PMMA opal templates after burning out PMMA microspheres. (a) well-formed inverse opal structure over large area, (b) enlarged view of the inverse opal showing individual $TiO_2$ nanoparticles. Black hole indicates the trace of necking between PMMA microspheres before calcinations.



of solution processible $TiO_2$ system, various applications towards photonic bandgap materials are underway.

In summary, the sol-gel $TiO_2$ nanoparticles synthesized in this study showed excellent stability in aqueous media due to the peptization process and the subsequent hydrothermal treatment. The suspensions were successfully spin coated onto the glass substrates exhibiting optically clean thin films with high refractive indices. An excellent solution processibility of $TiO_2$ suspensions developed in this study is expected to allow various photonic applications.

## Acknowledgments

Prof. Young Soo Seo in Sejong University is gratefully acknowledged for kind help with ellipsometry measurement. W. Lee and Y. G. Seo acknowledge the financial support by Renewable Energy Grant from KETEP (Grant No. 2008NPV08J 0130302008). K. Kim acknowledges the financial support by Renewable Energy Grant from KETEP (Grant No. 2008NPV08J010000). H. Lee acknowledges the financial support of this work by the National Research Foundation of Korea Grant funded by the Korean Government (MEST) (NRF-2009-C1AAA001-2009-0093049) and KIST internal project (2E20980).

## References

[1] Scolan, E. & Sanchez, C. (1998). *Chem. Mater.*, *10*, 3217–3223.
[2] Wang, Y., *et al.* (1999). *Thin Solid Films*, *349*, 120.
[3] Kay, A. & Gratzel, M. (1996). *Sol. Energy Mater. Sol. Cells*, *44*, 99–117.
[4] Kwak, E. S., *et al.* (2009). *Adv. Func. Mater.*, *19*, 1093–1099.
[5] Wang, C., Deng, Z.-X., & Li, Y. (2001). *Inorg. Chem.*, *40*, 5210–5214.
[6] Linsebigler, A. L., Lu, G., & Yates, J. T. (2002). *Chem. Rev.*, *95*, 735–758.
[7] Burnside, S. D., *et al.* (1998). *Chem. Mater.*, *10*, 2419–2425.
[8] Yang, S. C., *et al.* (2008). *Adv. Mater.*, *20*, 1059–1064.
[9] Yoon, J., *et al.* (2006). *Appl. Phys. Lett.*, *88*, 091102–091103.

[10] Kumar, K. N. P., *et al*. (1992). *Nature*, *358*, 48.
[11] Jeon, S. & Braun, P. V. (2003). *Chem. Mater.*, *15*, 1256–1263.
[12] Yanagisawa, K. & Ovenstone, J. (1999). *J. Phys. chem. B*, *103*, 7781.
[13] Yang, J., Mei, S., & Ferreira, J. M. F. (2000). *J. Am. Ceram. Soc.*, *83*, 1361.
[14] Egen, M. & Zentel, R. (2002). *Chem. Mater.*, *14*, 2176–2183.
[15] Joannopoulos, J. D., Meade, R. D., & Winn, J. N. (1995). *Photonic Crystals: Molding the Flow of Light*, Princeton University Press: Princeton.